

AD 681750

ERR-SD-051

*0*  
*OB*

ANALYTICAL INVESTIGATION OF FLOW DURATION  
IN THE CONVAIR HYPERSONIC SHOCK TUNNEL

by

C. J. Cohan

*583.0*  
*3760*  
*3385*

June 10, 1960

**DDC**  
**FEB 11 1969**  
**LIBRARY**

Engineering Research Report

This work was sponsored under Convair Research Program REA 9009

CONVAIR-  
ASTRONAUTICS  
JAN 16 1961  
LIBRARY

Distribution of this document  
is unlimited.



CONVAIR SAN DIEGO

CONVAIR DIVISION

GENERAL DYNAMICS CORPORATION



Theoretical Aerodynamics Note No. 33

ANALYTICAL INVESTIGATION OF FLOW DURATION IN THE CONVAIR HYPERSONIC SHOCK TUNNEL

SUMMARY

The analytical procedure used to calculate the steady flow duration in a hypersonic shock tunnel is presented. The results of this procedure applied to the Convaix Hypersonic Shock Tunnel are given. It is shown that for very low diaphragm pressure ratios,  $P_4^0/P_1^0 \lesssim 540$ , the steady flow duration is non-existent. For low diaphragm pressure ratios,  $540 \lesssim P_4^0/P_1^0 \lesssim 2000$ , which includes the tailored interface condition the steady flow duration is quite small. This is a result of pressure attenuation caused by the expansion waves reflected from the end of the driver.

Distribution of this document  
is unlimited.

Approved  
distribution is unlimited

SYMBOLS

$a$	Velocity of sound
$A$	area
$E_{ij}$	Dimensionless internal energy ratio
$g$	Equivalence factor [equation (2)]
$M$	Mach number
$p$	pressure
$P_{ij}$	Dimensionless pressure ratio $\frac{p_i}{p_j}$
$t$	Time
$u$	Particle velocity
$U_{ij}$	Dimensionless particle velocity $\frac{u_i}{a_j}$
$x$	Position along shock tube measured from diaphragm
$\gamma$	Ratio of specific heats, $\frac{c_p}{c_v}$
$\alpha$	$\frac{\gamma + 1}{\gamma - 1}$
$\beta$	$\frac{\gamma - 1}{2\gamma}$
$\rho$	Density
$R$	Rarefaction wave
$S$	Shock wave



## INTRODUCTION

The hypersonic shock tunnel is a development of the basic shock tube<sup>1</sup> in which the shock tube is used to produce a reservoir of high temperature, high pressure air which is expanded thru a nozzle to obtain the desired test conditions. Even though the shock tube is basically an unsteady flow device there are several regions in which the flow is steady and can be used as the reservoir. The durations of these steady flow regions in the basic shock tube are quite short, being of the order of a millisecond or less.

The steady flow duration of a hypersonic tunnel is determined by the duration of the steady state reservoir. The required flow duration may be about a millisecond for adequate measurement of pressure and heat transfer characteristics but should be two or three milliseconds for force measurements. Two modifications of the basic shock tunnel that have been developed to increase the available test time are the reflected shock design<sup>2</sup> and the tailored interface design.<sup>3</sup>

The duration of the steady flow reservoir and hence the test time available is a function of facility size and design as well as of the characteristics of the gases and initial pressure ratio used. This note will explain the analytical procedure used in calculating steady flow duration and will present the results of the flow duration analyses of the Convair Hypersonic Shock Tunnel.

## Discussion

### Wave Diagrams and Run Time

One of the most useful devices in analyzing shock tube flow is the wave diagram<sup>4,5</sup>. The wave diagram is a plot of the wave patterns in the  $x, t$ , plane where in the case of a shock tube,  $x$  is the longitudinal distance along the tube and  $t$  is the time. Figure 1 presents the wave diagram for a simple shock tube and the corresponding flow picture inside the tube at a time  $t_1$ .

Figure 2 compares wave diagrams for the simple shock tunnel, the reflected shock modification and the tailored interface technique. The available test time for each of these methods is also shown in Figure 2.

The simple shock tunnel,<sup>6</sup> merely has an expansion nozzle at the downstream end of the driven section. The available run time is basically the time difference between the arrival of the initial shock wave and the contact surface at the nozzle.

The most common modification to the basic shock tunnel is the reflected shock design in which the expansion nozzle is replaced by a conventional convergent-divergent nozzle.<sup>2</sup> The nozzle acts like a plate, almost completely reflecting the initial shock wave. The run time for this modification is the time difference between the arrival of the initial shock wave and the wave reflected from the contact surface.

The tailored interface shock tunnel is merely a special case of the reflected shock modification.<sup>3</sup> In this case the acoustic impedance is matched at the intersection of the reflected shock and the interface so that no wave is reflected from the interface. The available test time is the time difference

between the arrival of the initial shock wave and the unsteady expansion waves propagating downstream from the diaphragm.

These definitions of available test time assume that the expansion waves propagating upstream and reflecting from the end of the driver do not overtake the waves propagation downstream before the events described above take place.

#### Wave Diagram Construction

The method for constructing a wave diagram will be described for a shock tunnel with an area change at the diaphragm and a convergent-divergent nozzle at the end of the driven section. The wave diagram of such a tunnel is shown in Figure 3. Also shown in Figure 3 are the pressure distribution and wave picture along the tube at a time  $t$ .

The first step in constructing the wave diagram is a knowledge of the initial conditions in the driver and driven sections of the shock tube before rupture of the diaphragm. These include pressure, temperature speed of sound and the ratio of specific heats,  $\gamma$ . Given these initial conditions the pressure rise across the initial shock can be determined by an iterative procedure from the following equations for a shock tube with an area change at the diaphragm.<sup>7</sup>

$$P_{41} = \frac{P_{21}}{g} \left[ 1 - \frac{u_2}{a_1} \frac{a_1}{a_4} \frac{\gamma_4 - 1}{2} g - \frac{\gamma_4 - 1}{2\gamma_4} \right]^{-\frac{2\gamma_4}{\gamma_4 - 1}} \quad (1)$$

where  $g$  is an equivalence factor given by

$$g = \left\{ \left[ \frac{2 + (\gamma_4 - 1)M_{3a}^2}{2 + (\gamma_4 - 1)M_{3b}^2} \right]^{\frac{1}{2}} \left[ \frac{2 + (\gamma_4 - 1)M_{3b}^2}{2 + (\gamma_4 - 1)M_{3e}^2} \right] \right\}^{\frac{2\gamma_4}{\gamma_4 - 1}} \quad (2)$$

Since  $A_{3b}$  is the minimum section,  $M_{3b}$  is equal to unity but  $M_{3a}$  must still be determined in order to solve for  $g$  in equation (2).  $M_{3a}$  can be determined from the following equation since the area ratio  $\frac{A_4}{A_1}$  is known.

$$\frac{A_4}{A_1} = \frac{M_{3b}}{M_{3a}} \left[ \frac{2 + (\gamma_4 - 1)M_{3a}^2}{2 + (\gamma_4 - 1)M_{3b}^2} \right]^{\frac{\gamma_4 + 1}{2(\gamma_4 - 1)}} \quad (3)$$

For the Convair facility these equations have been solved for two initial driver conditions and the variation of initial shock pressure rise as a function of diaphragm pressure ratio is presented in Reference 8. This curve is reproduced herein as Figure 4.

Given the pressure rise  $\frac{P_2}{P_1}$  across the shock the other quantities across the shock can be obtained from the charts of Reference 9. The two quantities of immediate interest are the initial shock velocity  $U_S$  and the flow velocity  $u_2$  behind the shock. The flow velocity  $u_2$  is also the velocity of the interface or contact surface.

The pressure and particle velocity are the same on each side of the contact surface. Assuming the driver gas expands isentropically at a constant  $\gamma$ , the speed of sound of the driver gas at the contact surface can be found from

$$\frac{a_3}{a_4} = \left( \frac{P_3}{P_4} \right)^{\frac{\gamma_4 - 1}{2\gamma_4}} = \left( \frac{P_2}{P_4} \right)^{\frac{\gamma_4 - 1}{2\gamma_4}} = (P_{21} P_{14})^{\beta_4} \quad (4)$$

The initial shock reflects from the nozzle bringing the flow essentially to rest. The velocity of the reflected shock,  $U_{SR}$ , and the values of the thermodynamic properties behind the reflected shock are also obtained from Reference 9.

The flow behind the reflected shock is not brought completely to rest since there is outflow through the nozzle. The exact velocity in region 5 can be obtained by solving the continuity equation

$$\rho_5 A_5 u_5 = \rho_6 A_6 u_6 \quad (5)$$

An iterative procedure is used to find the conditions in region 6 which yield a Mach number of unity. The flow is assumed to expand isentropically from the reservoir with a negligible initial velocity,  $u_5$ . The Mollier diagram of Reference 10 is used to solve the energy equation.

$$h_5 = h_6 + \frac{u_6^2}{2} \quad (6)$$

The flow properties which satisfy equation (6) and yield a throat Mach number of unity are substituted into equation (5) and the actual reservoir velocity,  $u_5$ , is obtained.

The next step in constructing the wave diagram is calculating the interaction of the left running reflected shock wave and the right running contact surface. Such interactions are discussed in References 4 and 5. In general the interaction will result in both a transmitted wave and a reflected wave. The type of reflected wave depends on the shock strength,  $P_{52}$ , and the internal energy ratio,  $E_{32}$ .

For the case of a reflected shock wave<sup>5</sup>

$$E_{32} = \frac{\alpha_3 + P_{25} P_{57} h}{1 - P_{25} P_{57}} \left[ k \sqrt{P_{57}} - \frac{P_{57} - 1}{\alpha_2 + P_{57}} \right] \quad (7)$$

where  $h = \frac{\alpha_2 P_{25} + 1}{\alpha_2 + P_{25}} \quad (8a)$

$$k = \frac{1 - P_{25}}{\sqrt{\alpha_2 P_{25} + 1}} \quad (8b)$$

$$E_{32} \leq \frac{\alpha_3 + P_{25}}{\alpha_2 + P_{25}} \quad (8c)$$

The use of a reflected rarefaction wave is given by

$$P_{75}^{\beta_2} + f(P_{75} - P_{25}) \sqrt{\frac{\beta_2 E_{32}}{\alpha_3 P_{75} + P_{25}}} - \bar{g} - 1 = 0 \quad (9)$$

where  $f = \left[ \frac{\alpha_2 + P_{25}}{\alpha_2 P_{25} + 1} \right]^{\frac{1}{2}}$  (10a)

$$\bar{g} = (1 - P_{25}) \left[ \frac{\beta_2}{\alpha_2 P_{25} + 1} \right]^{\frac{1}{2}} \quad (10b)$$

$$E_{15} \geq \frac{\alpha_3 + P_{25}}{\alpha_2 + P_{25}} \quad (10c)$$

Relations (8c) and (10c) determine the type of reflected wave. Equations (7) or (9) can be used to calculate the pressure ratio across the reflected wave. This pressure ratio can be used to calculate the flow velocity after the wave from the following equations<sup>11</sup>

$$\frac{u_7}{a_5} = M_5 + \frac{1}{\gamma \bar{g}} \left[ P_{75}^{\beta_2} - 1 \right] \text{ for a rarefaction wave} \quad (11)$$

or  $\frac{u_7}{a_5} = M_5 + \frac{P_{75} - 1}{\gamma \sqrt{\beta_2 (\alpha_3 P_{75} + 1)}} \text{ for a shock wave} \quad (12)$

In using equations (7) through (12) the assumption is made that the value of  $\gamma$  for each gas does not change across the reflected wave.

A special case of this interaction between the shock wave and the contact surface occurs when the following relation is satisfied

$$E_{15} = \frac{\alpha_3 + P_{25}}{\alpha_2 + P_{25}} \quad (13)$$

This is the tailored interface condition in which there is no reflected wave. Since there is no reflected wave from the contact surface the following relations must also be satisfied.<sup>1</sup>

$$P_3 = P_5 \tag{14}$$

$$u_8 = u_5$$

so therefore

$$\frac{P_8}{P_3} = \frac{P_5}{P_2} = \bar{P} \tag{15}$$

$$u_5 - u_2 = u_8 - u_3$$

the change in velocity across a shock is given by

$$\frac{\Delta u}{a} = \left[ \frac{2}{\gamma(\gamma-1)} \right]^{\frac{1}{2}} \frac{\bar{P} - 1}{1 + \alpha \bar{P}^2} \tag{16}$$

Combining equations (15) and (16) gives

$$\frac{\gamma_2(\gamma_2 - 1)(1 + \alpha_2 \bar{P})}{a_2^2} = \frac{\gamma_3(\gamma_3 - 1)(1 + \alpha_3 \bar{P})}{a_3^2} \tag{17}$$

which must be satisfied if there is to be no reflected wave.

The driver gas expands to the conditions in region 3 through two unsteady expansions and one steady expansion. The slope of an expansion wave,  $\frac{dx}{dt}$ , in the x,t plane is given by

$$\frac{dx}{dt} = u - a \text{ for a left running wave} \tag{18}$$

$$\frac{dx}{dt} = u + a \text{ for a right running wave} \tag{19}$$

In order to construct the wave diagram it is therefore necessary to know the velocity, u, and the speed of sound, a, at each point of interest. For a non

steady expansion<sup>12</sup>

$$\frac{2}{\gamma - 1} a_i^2 + u_i^2 = \frac{2}{\gamma - 1} a_j^2 + u_j^2 \quad (20)$$

For a steady expansion

$$\frac{2}{\gamma - 1} c_i^2 + u_i^2 = \frac{2}{\gamma - 1} a_j^2 + u_j^2 \quad (21)$$

and since all expansions are adiabatic

$$\frac{a_i}{a_j} = \left( \frac{P_i}{P_j} \right)^{\frac{\gamma - 1}{2\gamma}} \quad (22)$$

Equations (18) through (22) can be used to calculate the flow velocity and speed of sound at any point in the initial expansion wave flow field.

The last wave of interest in constructing a wave diagram to determine steady flow duration is the rarefaction wave reflected from the end of the driver. The propagation of this wave is calculated using the flow properties determined from the initial expansion wave analysis described above. This reflected rarefaction wave is a right running wave so the velocity of propagation is given by equation (19).

## RESULTS

The above method of constructing wave diagrams has been applied to the Convair Hypersonic Shock Tunnel for two sets of initial conditions using the theoretical initial shock wave data of Figure 4. One of these initial conditions is for a relatively low diaphragm pressure ratio,  $P_{41} = 540$ , and the other is for a tailored interface condition of higher pressure ratio. The exact initial conditions and the resulting wave diagrams are presented in Figures 5 and 6. These wave diagrams have been computed for both the present

driver, length 5.4 ft., and for a driver extended to 13.1 ft. so that two reflected rarefaction waves are shown in each figure. For clarity the effect of the rarefaction wave reflected from the end of the present driver upon the other waves in the shock tube has not been shown. It is readily seen in Figures 5 and 6 that the reflected rarefaction wave in the present driver will attenuate the reservoir pressure and therefore lead to a time gradient of dynamic pressure at the model.

Figure 7 shows steady flow duration as a function of shock Mach number with cut off lines for three driver lengths. It will be seen that the present driver length reduces the steady flow duration for  $M_s = 9.7$ . The effect of this in reducing the operating range of the tunnel is shown in Figure 8. It appears that steady simulation of conditions below 15,000 ft./sec. would be eliminated.

In Figure 7 the tailored interface condition is shown as being achievable over only a very narrow band of shock Mach numbers. In practice, however, the shock waves and expansion waves reflected from the contact surface for a band of shock Mach numbers near this condition should not be sufficiently strong to effect the flow over the model significantly. Therefore, the tailored interface concept may be effective if good control of shock velocity is attained.

If an 8 ft. extension is made to the driver, the maximum tailored interface flow duration may be obtained as well as virtually eliminating the limits on the reflected shock case.

A decision on the length of extension to be selected should be based on flow duration measurements in the facility since at least two uncertainties

**CONVAIR**  
A DIVISION OF GENERAL DYNAMICS CORPORATION  
SAN DIEGO

PAGE 12  
EDEC AERO NOTE 33  
DATE 6/10/60

apply to these calculations. The speed of sound in the driver gas has been obtained by thermodynamic calculations of the combustion process and may be in considerable error. Also no allowance has been made for shock attenuation due to viscous effects in the driven section.

Prepared by *C. J. Cohan*  
C. J. Cohan

Checked by *R. E. Fowler*  
~~R. E. Fowler~~

Approved by *H. Yoshihara*  
H. Yoshihara  
Chief, Fluid Dynamics  
Research



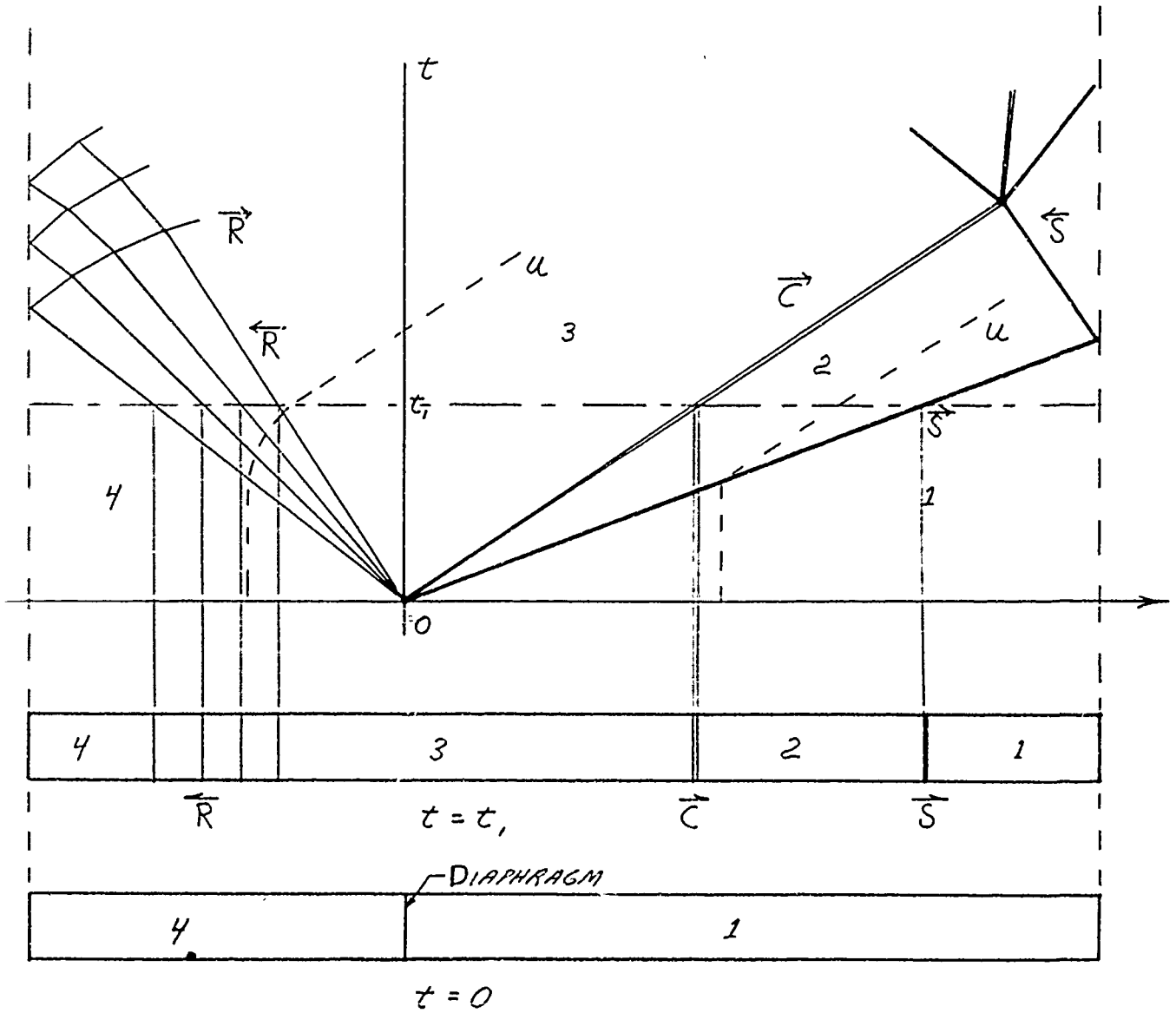
#### REFERENCES

1. Martin, W. A., "A Review of Shock Tubes and Shock Tunnels", Convair, San Diego, Aerodynamics Report ZA-280, September 10, 1958.
2. Hertzberg, A., Smith, W. E., Glick, H. S., and Squire, W., "Modifications of the Shock Tube for the Generation of Hypersonic Flow". C.A.L. Report No. AD-739-A-2, AEDC TN 55-15, AD63559, March 1955.
3. Wittliff, C. E., Wilson, M. R., and Hertzberg, A., "The Tailored Interface Hypersonic Shock Tunnel". C.A.L. Report No. AD-1052-A-8.
4. Rudinger, G., "Wave Diagrams for Nonsteady Flow in Ducts". Van Nostrand, New York, 1955.
5. Glass, I. I., "Shock Tubes: Part I; Theory and Performance of Simple Shock Tubes", U.T.I.A. Review No. 12, May, 1958.
6. Hertzberg, A., "A Shock Tube Method for Generating Hypersonic Flows", JAS, Vol. 18, 1951.
7. Alpher, R. A. and White, D. R., "Flow in Shock Tubes with Area Change at the Diaphragm Station, J. of Fluid Mechanics, Vol. 6, Part 3, February 1958.
3. Martin, W. A., "Initial Calibration of the Convair Hypersonic Shock Tunnel", Convair, San Diego, Theoretical Aerodynamics Note No. 25.
9. Cohan, C. J., "Shock Tube Performance Charts for Moving and Reflected Normal Shocks", Convair, San Diego, Theoretical Aerodynamics Note No. 31, May 26, 1960.
10. Feldman, S., "Hypersonic Gas Dynamic Charts for Equilibrium Air", AVCO Research Laboratory, January, 1957.

11. Glass, I. I., "On the One Dimensional Overtaking of a Shock Wave by a Rarefaction Wave", U.F.I.A. Technical Note No. 30, July 1959.
12. Russo, A. L., and Hertzberg, A., "Modifications of the Basic Shock Tube to Improve its Performance", C.A.L. Report No. AD-1052-A-7, August 1958.

WAVE DIAGRAM FOR A SIMPLE SHOCK TUBE

FIGURE 1



1 = DRIVEN SECTION  
 4 = DRIVER SECTION  
 R = RAREFACTION WAVE

S = SHOCK WAVE  
 C = CONTACT SURFACE  
 U = PARTICLE PATH

WAVE DIAGRAMS AND STEADY FLOW DURATIONS  
FOR VARIOUS SHOCK TUNNEL DESIGNS

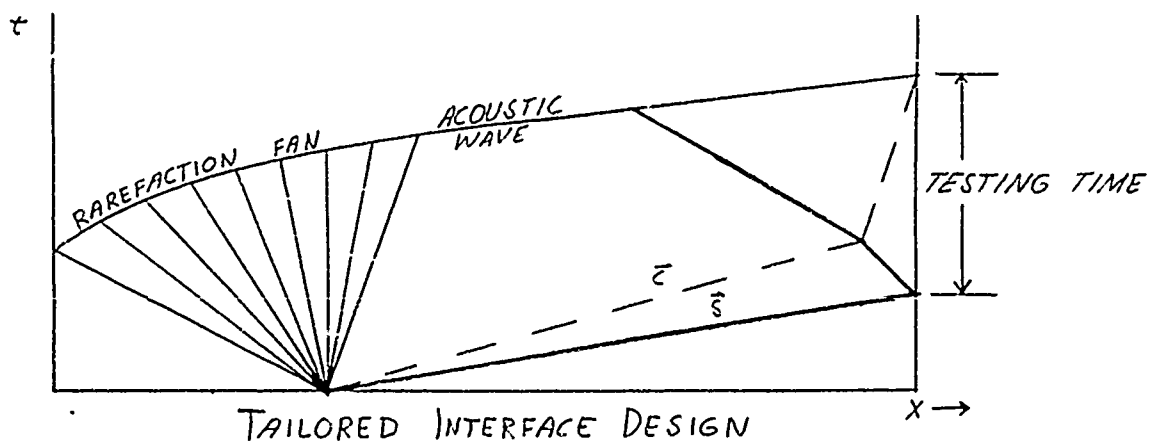
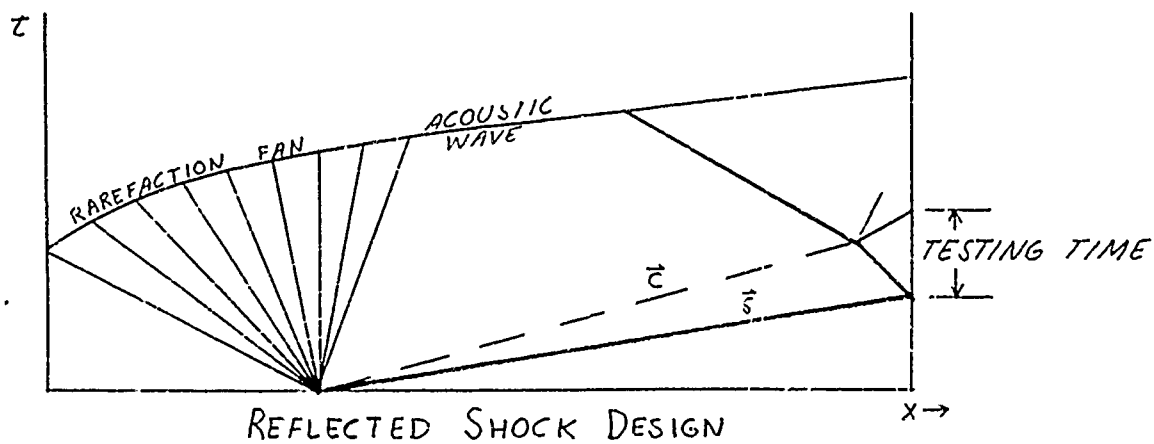
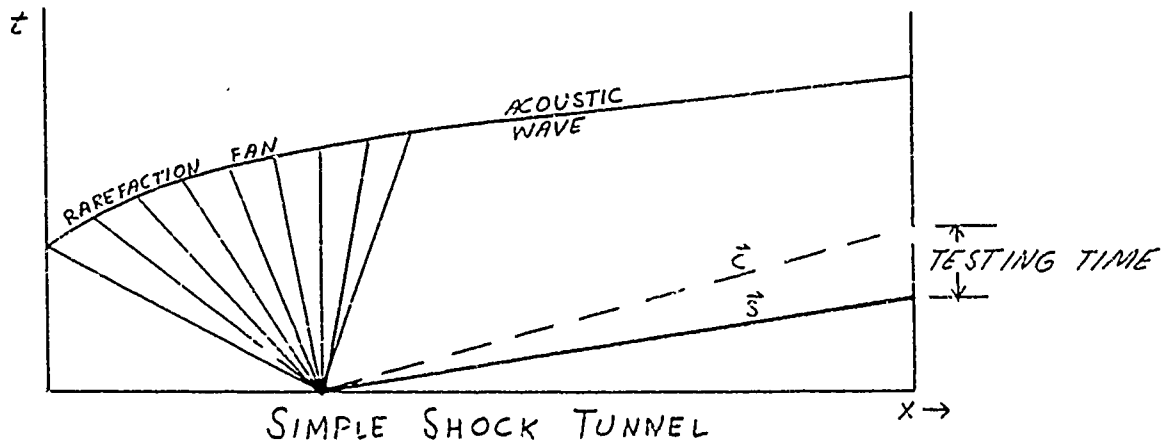
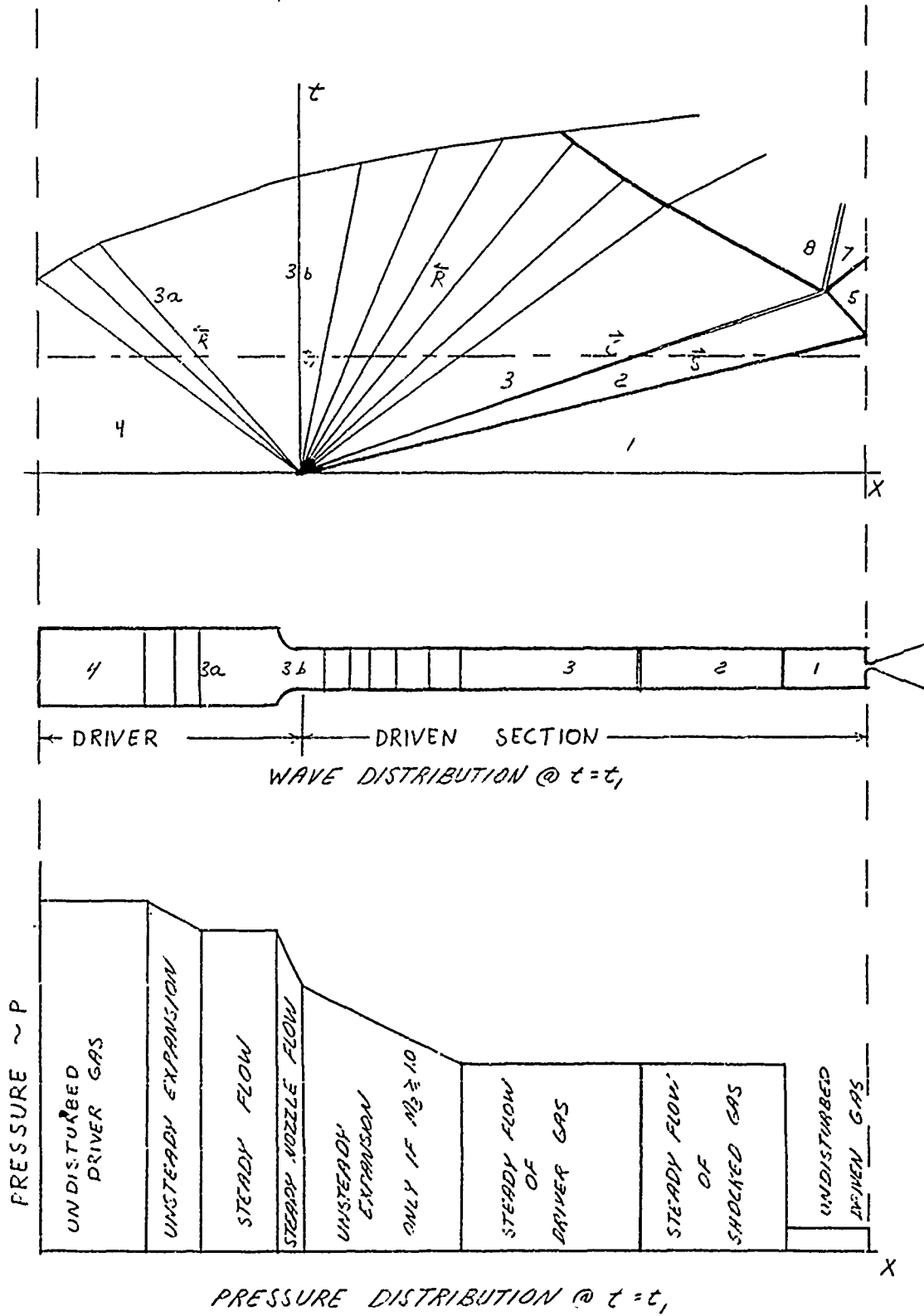


FIGURE 2

SHOCK TUNNEL WAVE DIAGRAM & PRESSURE DISTRIBUTION

FIGURE 3



A

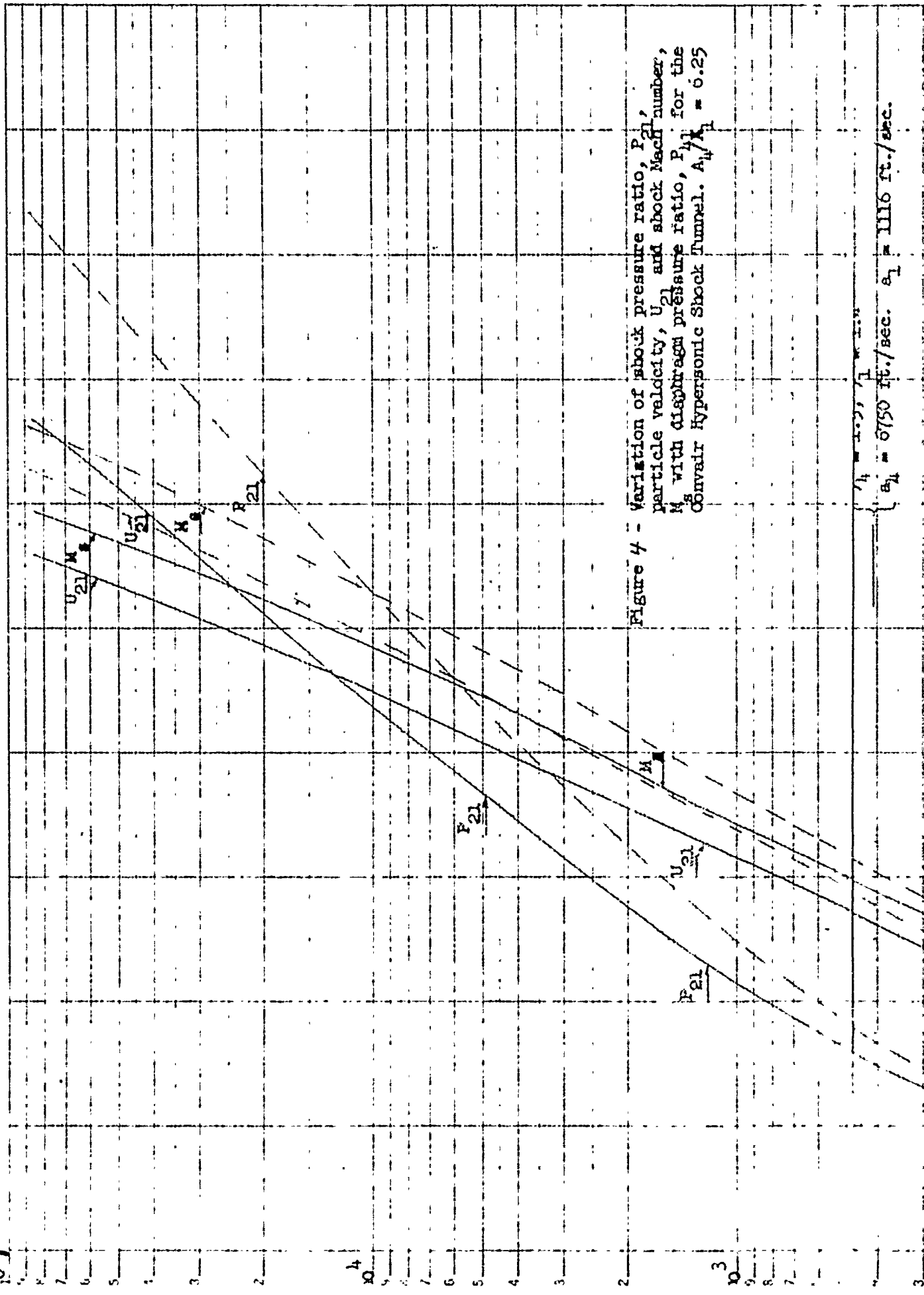
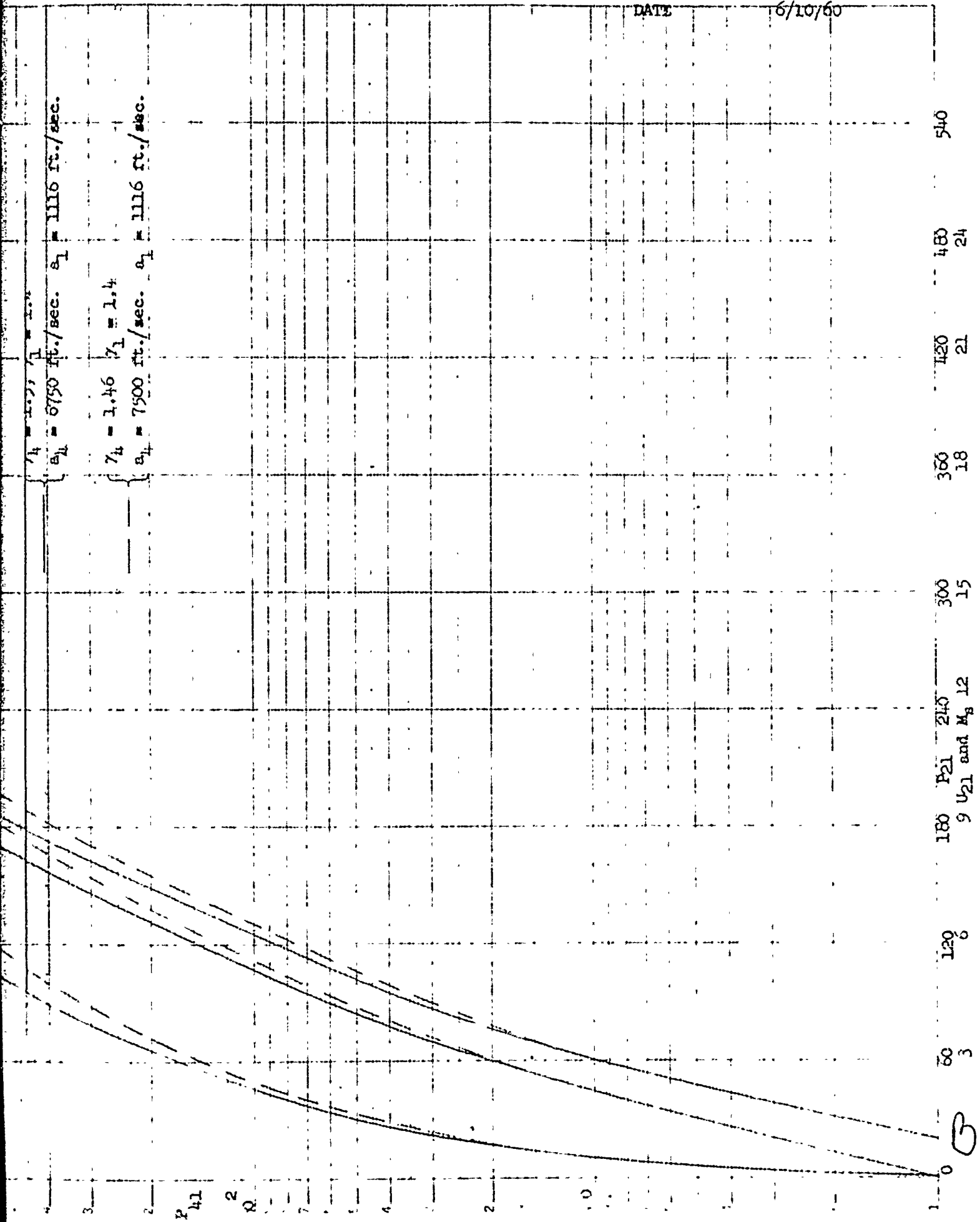


Figure 4 - Variation of shock pressure ratio,  $P_{21}$ , particle velocity,  $U_{21}$  and shock Mach number,  $M_s$  with upstream pressure ratio,  $P_{11}$  for the Convair Hypersonic Shock Tunnel.  $A_1/A_2 = 6.25$

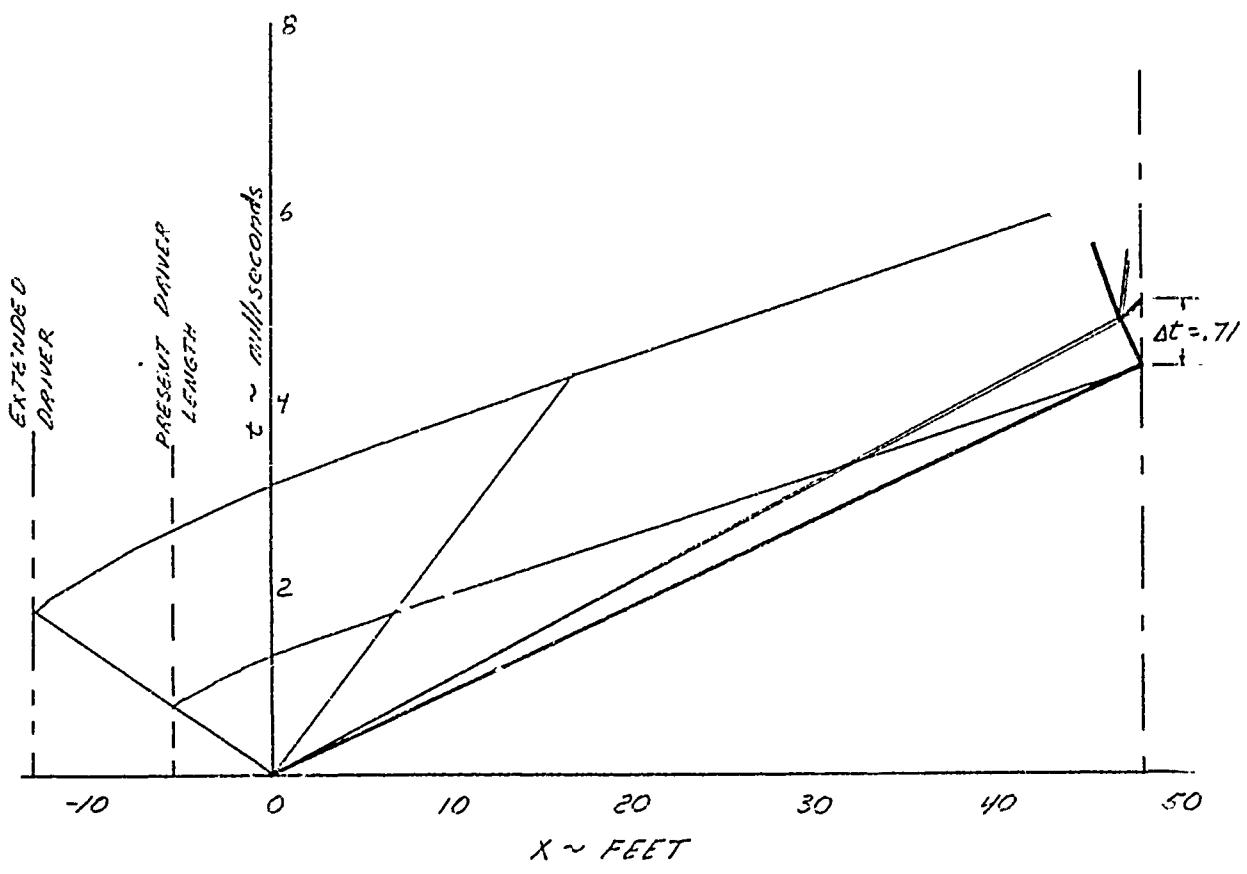
$\gamma_4 = 1.46$   
 $\gamma_1 = 1.4$   
 $a_4 = 6750 \text{ ft./sec.}$   
 $a_1 = 1116 \text{ ft./sec.}$



180  $P_{21}$  240 300 360 420 480 540  
 9  $U_{21}$  and  $M_3$  12 15 18 21 24

CONVAIR HYPERSONIC SHOCK TUNNEL  
WAVE DIAGRAM  
THEORETICAL SHOCK TUBE PERFORMANCE  
 FIGURE 5

INITIAL CONDITIONS  
 $P_1 = 2 \text{ Atm.}$        $P_4 = 16,000 \text{ ps i.}$   
 $T_1 = 300^\circ \text{K}$        $a_4 = 7500 \text{ ft/sec.}$   
 $\gamma_1 = 1.4$        $\gamma_4 = 1.46$   
 $P_4/P_1 = 545$

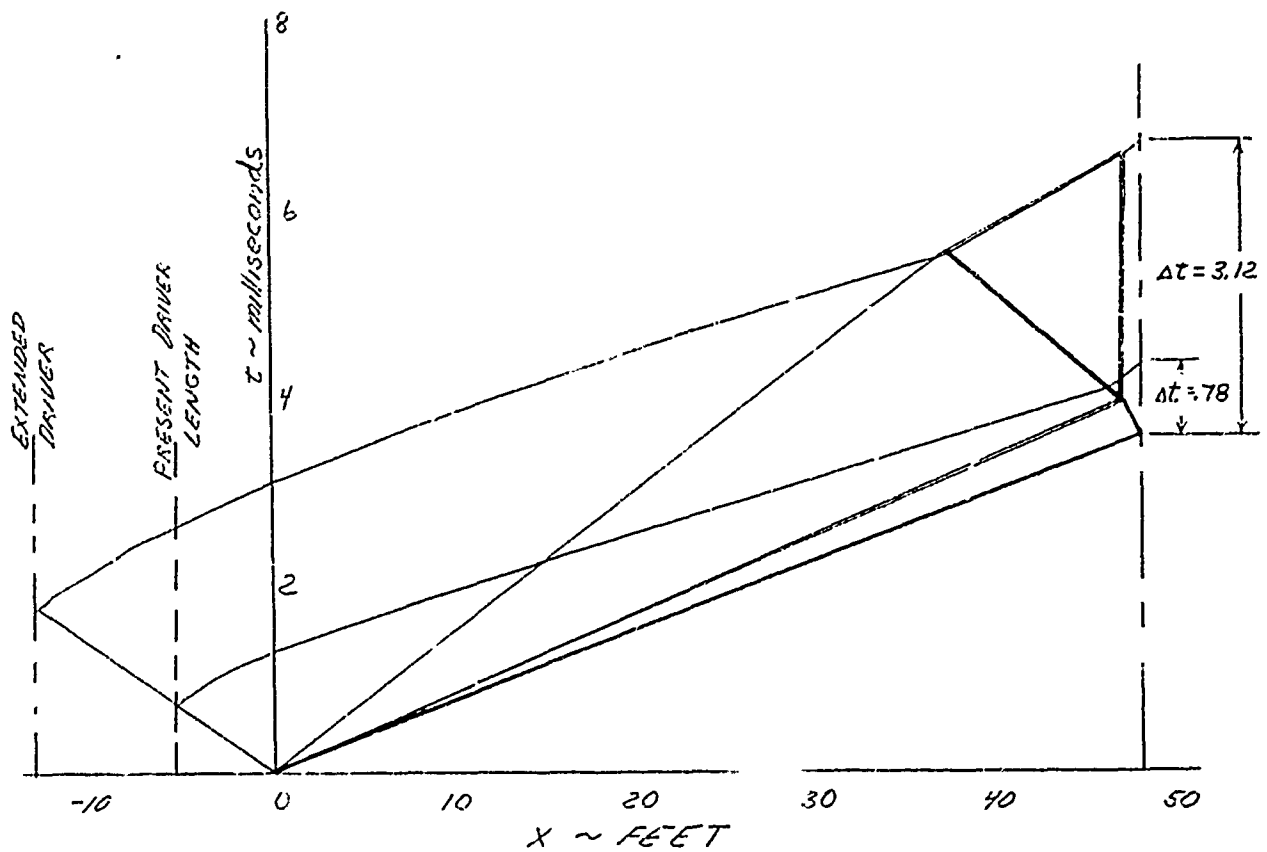


PRESENT DRIVER LENGTH = 54 ft.  
PRESENT DRIVEN LENGTH = 48 ft.  
EXTENDED DRIVER LENGTH = 121 ft  
FLOW DURATION,  $\Delta t$ , IN MILLISECONDS

CONVAIR HYPERSONIC SHOCK TUNNEL  
TAILORED INTERFACE CONDITION WAVE DIAGRAM  
THEORETICAL SHOCK TUBE PERFORMANCE

FIGURE 6

INITIAL CONDITIONS	
$P_1 = 1 \text{ Atm.}$	$P_4 = 1470 \text{ Atm}$
$T_1 = 300^\circ\text{K}$	$a_4 = 7500 \text{ ft/sec.}$
$\gamma_1 = 1.4$	$\gamma_4 = 1.46$

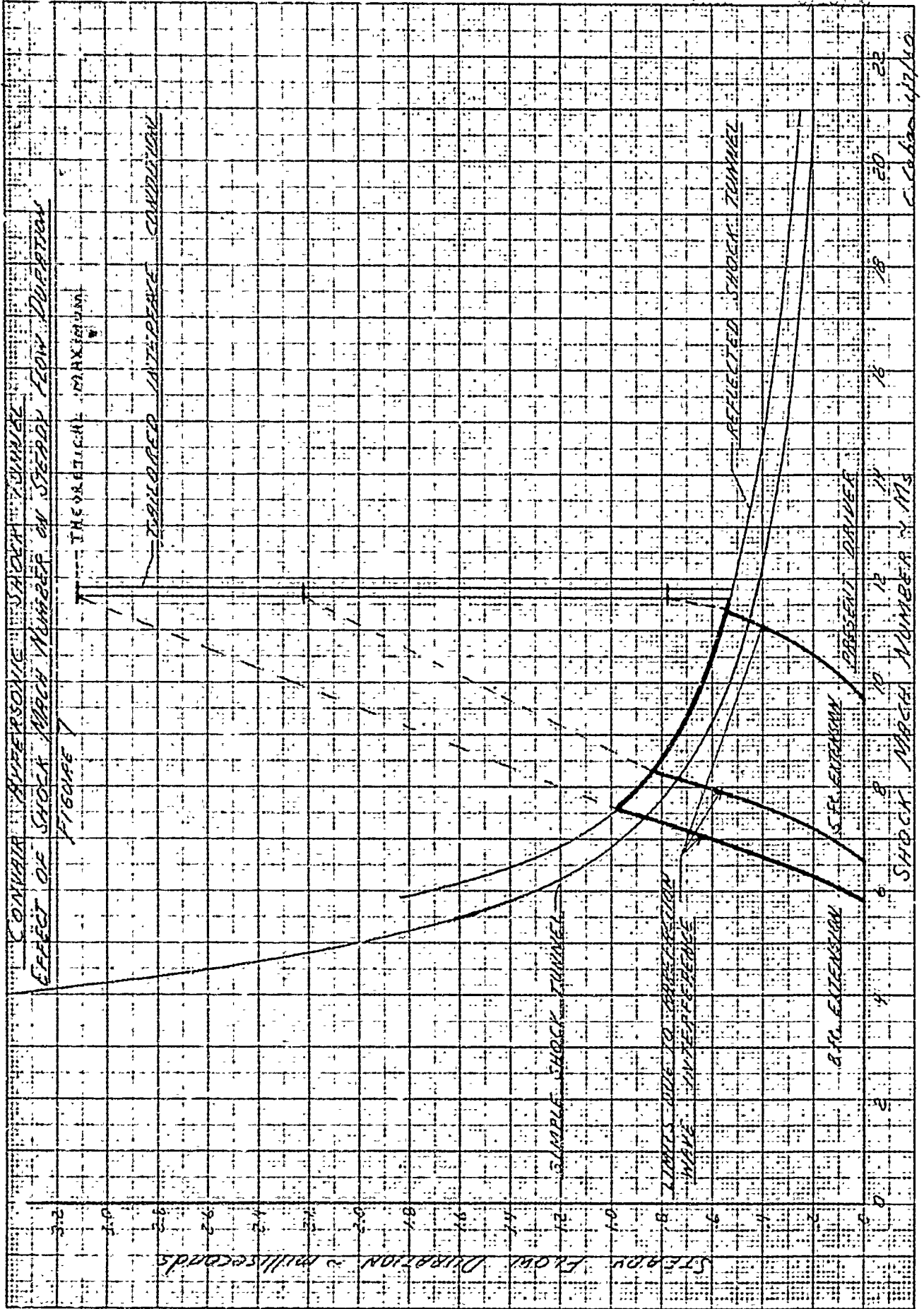


PRESENT DRIVER LENGTH = 5.4 ft

PRESENT DRIVEN LENGTH = 48 ft.

EXTENDED DRIVER LENGTH = 13.1 ft.

FLOW DURATION, Δt, IN MILLISECONDS



C. Coburn 4/7/40

